

1 Conference Proceedings Paper

2 Photoconductivity of the Single Crystals 3 $\text{Pb}_4\text{Ga}_4\text{GeS}_{12}$ and $\text{Pb}_4\text{Ga}_4\text{GeSe}_{12}$

4 Hadj Bellagra¹, Oksana Nyhmatullina², Yuri Kogut¹, Halyna Myronchuk², Lyudmyla Piskach^{1*}

5 ¹ Eastern European National University, Department of Chemistry, Voli Ave. 13, Lutsk 43025, Ukraine

6 ² Eastern European National University, Department of Physics, Voli Ave. 13, Lutsk 43025, Ukraine

7 * Correspondence: lyuda0760@ukr.net; Tel.: +380-50-911-1265

8 Published: 6 November 2020

9 **Abstract:** Quaternary semiconductor materials of the $\text{Pb}_4\text{Ga}_4\text{GeS}(\text{Se})_{12}$ composition have attracted
10 the attention of researchers due to possible use as active elements of optoelectronics and nonlinear
11 optics. The $\text{Pb}_4\text{Ga}_4\text{GeS}(\text{Se})_{12}$ phases belong to the solid solution ranges of the $\text{Pb}_3\text{Ga}_2\text{GeS}(\text{Se})_8$
12 compounds which form in the quasi-ternary systems $\text{PbS}(\text{Se})-\text{Ga}_2\text{S}(\text{Se})_3-\text{GeS}(\text{Se})_2$ at the cross of the
13 $\text{PbGa}_2\text{S}(\text{Se})_4-\text{Pb}_2\text{GeS}(\text{Se})_4$ and $\text{PbS}(\text{Se})-\text{PbGa}_2\text{GeS}(\text{Se})_6$ sections. The quaternary sulfide melts
14 congruently at 943 K. The crystallization of the $\text{Pb}_4\text{Ga}_4\text{GeSe}_{12}$ phase is associated with the ternary
15 peritectic process $L_p + \text{PbSe} \leftrightarrow \text{PbGa}_2\text{S}_4 + \text{Pb}_3\text{Ga}_2\text{GeSe}_8$ at 868 K. For the single crystal studies,
16 $\text{Pb}_4\text{Ga}_4\text{GeS}(\text{Se})_{12}$ were pre-synthesized by co-melting high-purity elements. X-ray diffraction results
17 confirm that these compounds possess non-centrosymmetric crystal structure (tetragonal
18 symmetry, space group $P\bar{4}2_1c$). The crystals were grown by the vertical Bridgman method in a two-
19 zone furnace. The starting composition was stoichiometric for $\text{Pb}_4\text{Ga}_4\text{GeS}_{12}$, and the solution-melt
20 method was used for the selenide $\text{Pb}_4\text{Ga}_4\text{GeSe}_{12}$. Obtained value of the bandgap energy for the
21 $\text{Pb}_4\text{Ga}_4\text{GeS}_{12}$ and $\text{Pb}_4\text{Ga}_4\text{GeSe}_{12}$ crystals is 1.86 and 2.28 eV, respectively. Experimental
22 measurements of the spectral distribution of photoconductivity for the $\text{Pb}_4\text{Ga}_4\text{GeS}_{12}$ and
23 $\text{Pb}_4\text{Ga}_4\text{GeSe}_{12}$ crystals exhibit the presence of two spectral maxima. The first lies in the region of 570
24 nm (2.17 eV) and 680 nm (1.82 eV), respectively, and matches well the optical bandgap estimates.
25 The locations of the admixture maxima at about 1030 nm (1.20 eV) and 1340 nm (0.92 eV),
26 respectively, agree satisfactorily with the calculated energy positions of the defects V_s and V_{Se} .

27 **Keywords:** quaternary chalcogenides; phase equilibria; single crystals; photoconductivity

29 1. Introduction

30 Recently, series of new compounds were discovered (4-4-1-12 type: $\text{Pb}_4\text{Ga}_4\text{Ge}(\text{S},\text{Se})_{12}$ [1], and 1-
31 2-1-6 type: $\text{PbGa}_2\text{Ge}(\text{Si})\text{Se}_6$, $\text{SnGa}_2\text{Ge}(\text{S},\text{Se})_6$, $\text{PbGa}_2\text{GeS}_6$ [2-5]) that possess qualitatively new physical
32 properties and may serve as a basis for the design of non-linear optical materials. The 4-4-1-12
33 quaternary compounds feature non-linear coefficients exceeding those of $\text{AgGa}(\text{S},\text{Se})_2$ (record second
34 harmonic generation (SHG) efficiencies) and an order of magnitude higher laser damage threshold.
35 Additionally, they have much longer-wave limit of IR transparency (up to 23 μm) and more suitable
36 double refraction for phase synchronism of the converted radiation in the 1–10 μm range. The authors
37 [1] report that the $\text{Pb}_4\text{Ga}_4\text{GeS}(\text{Se})_{12}$ compounds are isostructural and crystallize in the tetragonal
38 symmetry, space group $P\bar{4}2_1c$, with the unit cell parameters $a=1.2673(2)$, $c=0.6128(2)$ nm for
39 $\text{Pb}_4\text{Ga}_4\text{GeS}_{12}$, and $a=1.3064(7)$, $c=0.6310(5)$ nm for $\text{Pb}_4\text{Ga}_4\text{GeSe}_{12}$. They have bandgap energy of 2.35
40 and 1.91 eV and are transparent in wide range of IR spectrum 0.80–22.5 and 0.75–22.5 μm ,
41 respectively.

42 Our research was focused on the technology of the single crystal growth of these compounds,
43 and their possible use in active elements for linear and non-linear optics and optoelectronics.

44 2. Materials and Methods

45 Polycrystalline alloys of the $\text{Pb}_4\text{Ga}_4\text{GeS}(\text{Se})_{12}$ compositions were preliminarily synthesized by com-
46 melting the elements in stoichiometric ratio. The batches were composed of high-purity elements Pb,
47 99.99 wt.%, Ga, 99.9997% (SmiLab Ltd), Ge, 99.9999 wt.%, S, Se 99.999 wt.% (Alfa Aesar). Lead was
48 additionally purified by dripping through crushed quartz under static conditions. The total batch
49 mass was 20 g. The sulfur-containing quartz ampoule was evacuated to 10^{-2} Pa and was locally heated
50 in the oxygen-gas burner flame to complete bonding of sulfur under visual observation of the reaction
51 process. Considering high vapor pressure, $\text{Pb}_4\text{Ga}_4\text{GeS}_{12}$ was synthesized in 5 g batches followed by
52 the transfer of the powdered obtained alloy to the growth container. $\text{Pb}_4\text{Ga}_4\text{GeSe}_{12}$ was synthesized
53 already in the evacuated growth container. Quartz ampoules with conical bottom were used for the
54 crystal growth.

55 The results of preliminary experiments suggest critical importance of the homogeneity of the
56 starting batch and rather high temperature gradient at the solid-melt interface. This is because lead
57 reacts rather poorly with chalcogens. Initial interaction of the elements yields binary lead
58 chalcogenide which surrounds molten lead and prevents further reaction with other elements or
59 binary chalcogenides of other metals. Additionally, the melts of these systems have high viscosity as
60 one of the system components ($\text{GeS}(\text{Se})_2$) is a known glass-forming agent. High viscosity hinders
61 diffusion mixing of the melt above the growing crystal which may lead to the formation of blocs,
62 admixtures of other phases, uncontrolled occlusion, all of which affect the properties of single
63 crystals. Therefore, operations of forced homogenization are necessary, such as furnace rotation or
64 vibration, or crushing the alloy into powder before loading it in the growth container.

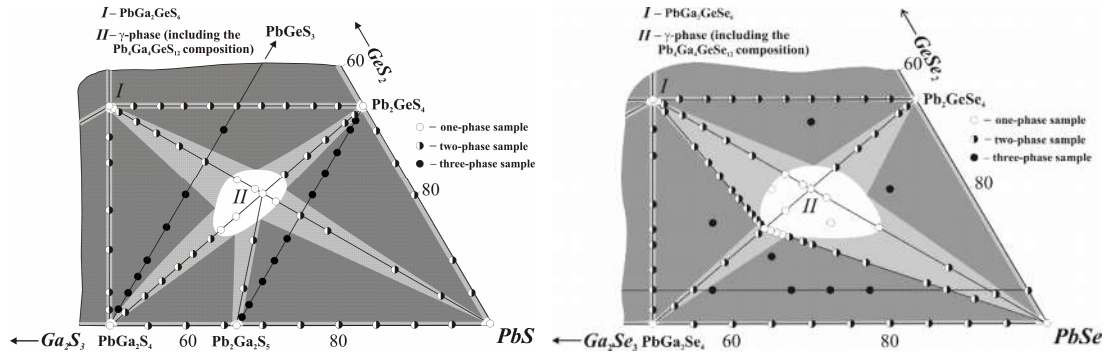
65 Homogenization of the alloys of both phases was achieved by placing the ampoules with the
66 alloys in a rotation furnace and heating to 1170 K at the rate of 50 K/hr. The furnace was rotated at
67 this temperature for 24 hrs. after stopping the furnace in the vertical position, the alloys were cooled
68 at 20 K/hr to 670 K, and annealed for 240 hrs. The synthesis process was finished by cooling to room
69 temperature in the inertial mode. Obtained alloys were compact ingots.

70 The crystal growth was performed by Bridgman method [6] in a two-zone furnace with steady
71 temperature profile. The growth containers with the synthesized batches were placed in the pre-
72 heated furnace. The temperature of the upper isothermal zone was 1170 K, the lower zone varied
73 within 620 to 670 K. The temperature in the growth zone was controlled with ± 0.5 K accuracy.
74 Independent temperature control and selection of metal discs between the two zones permitted the
75 variation of temperature gradient at the solid-melt interface of 1.2–3 K/cm. The growth rate varied in
76 the range of 5–6 mm/day. After the complete crystallization of the melts, the furnace was cooled to
77 room temperature at the rate of 5 K/hr.

78 3. Results

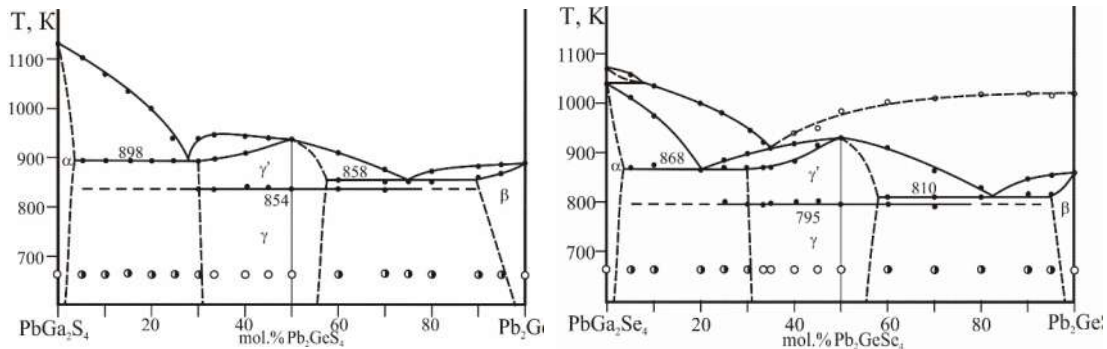
79 3.1. Phase equilibria related to the formation of $\text{Pb}_3\text{Ga}_2\text{GeS}(\text{Se})_8$

80 Our investigations of the quasi-ternary systems $\text{PbS}(\text{Se})\text{--Ga}_2\text{S}(\text{Se})_3\text{--GeS}(\text{Se})_2$ by XRD and DTA
81 methods (to be published in detail elsewhere) showed that the $\text{Pb}_4\text{Ga}_4\text{GeS}(\text{Se})_{12}$ compositions belong
82 to the solid solution ranges of the $\text{Pb}_3\text{Ga}_2\text{GeS}(\text{Se})_8$ compounds that form at the crossing of the sections
83 $\text{PbGa}_2\text{S}(\text{Se})_4\text{--Pb}_2\text{GeS}(\text{Se})_4$ and $\text{PbS}(\text{Se})\text{--PbGa}_2\text{GeS}(\text{Se})_6$ (Figure 1).



84 **Figure 1.** Isothermal sections of the $\text{PbS(Se)-Ga}_2\text{S(Se)}_3\text{-GeS(Se)}_2$ systems in the
85 $\text{PbS(Se)-Pb}_2\text{GeS(Se)}_4\text{-PbGa}_2\text{GeS(Se)}_6\text{-PbGa}_2\text{S(Se)}_4$ part at 670 K.

86 Vertical sections $\text{PbGa}_2\text{S(Se)}_4\text{-Pb}_2\text{GeS(Se)}_4$ were investigated to consider the conditions for the
87 crystal growth of $\text{Pb}_4\text{Ga}_4\text{GeS(Se)}_{12}$ as the sections demonstrate the nature of the formation of these
88 phases (Figure 2). The sulfur-containing section $\text{PbGa}_2\text{S}_4\text{-Pb}_2\text{GeS}_4$ is quasi-binary in the entire
89 concentration and temperature range, while the selenide section $\text{PbGa}_2\text{Se}_4\text{-Pb}_2\text{GeSe}_4$ is quasi-binary
90 only in the sub-solidus region due to incongruent melting of the starting ternary compounds
91 PbGa_2Se_4 and Pb_2GeSe_4 . Each of the 4-4-1-12 compounds is dimorphous, with the phase transitions
92 taking place at 854 K for the sulfide and 795 K for the selenide. The $\text{Pb}_4\text{Ga}_4\text{GeS(Se)}_{12}$ phases each
93 occupies at the studied sections $\text{PbGa}_2\text{S(Se)}_4\text{-Pb}_2\text{GeS(Se)}_4$ the range of ~32–57 mol.% $\text{Pb}_2\text{GeS(Se)}_4$.
94



95 **Figure 2.** Phase diagrams of the $\text{PbGa}_2\text{S(Se)}_4\text{-Pb}_2\text{GeS(Se)}_4$ systems.

96 The quaternary sulfide melts congruently at 943 K. The melting point maximum falls onto the
97 $\text{Pb}_4\text{Ga}_4\text{GeS}_{12}$ composition, while the stoichiometric composition of the quaternary solid solution
98 corresponds to $\text{Pb}_3\text{Ga}_2\text{GeS}_8$. The eutectic between PbGa_2S_4 and HT- $\text{Pb}_4\text{Ga}_4\text{GeS}_{12}$ lies at 27 mol.%
99 Pb_2GeS_4 , 898 K; the eutectic between HT- $\text{Pb}_4\text{Ga}_4\text{GeS}_{12}$ and Pb_2GeS_4 is at 75 mol.% Pb_2GeS_4 , 858 K.

100 The crystallization of the $\text{Pb}_4\text{Ga}_4\text{GeS}_{12}$ phase is related to the ternary peritectic process $\text{Lp}_1 +$
101 $\text{PbSe} \rightleftharpoons \text{PbGa}_2\text{Se}_4$ (α -solid solutions) + $\text{Pb}_3\text{Ga}_2\text{GeSe}_8$ (γ -solid solutions) at 868 K in the
102 $\text{PbSe-Ga}_2\text{Se}_3\text{-GeSe}_2$ system. The other ternary peritectic process $\text{Lp}_2 + \text{PbSe} \rightleftharpoons \text{Pb}_3\text{Ga}_2\text{GeSe}_8$ (γ -solid
103 solutions) + Pb_2GeSe_4 (β -solid solutions) takes place at 810 K.

104 3.2. Optical properties of the $\text{Pb}_3\text{Ga}_2\text{GeS(Se)}_8$ single crystals

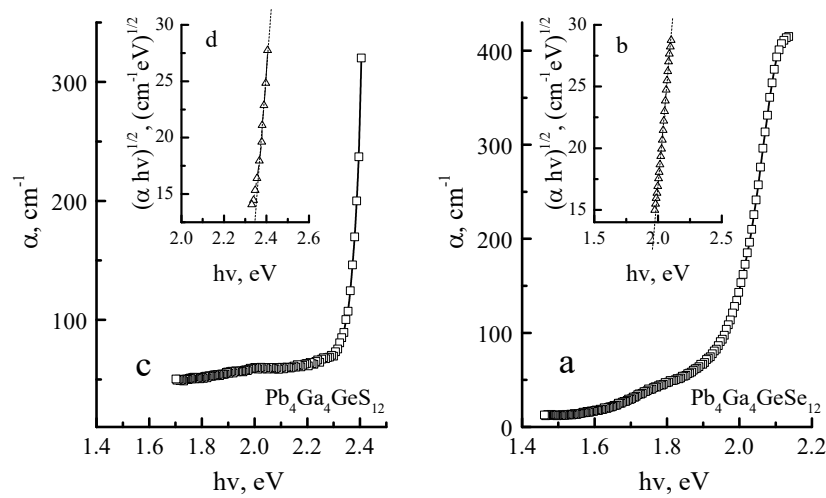
105 Two experiments of the growth of each of the crystals were performed. The increase of the
106 temperature gradient proved quite advantageous. Using optimized growth condition, crystals of up
107 to 11 mm diameter and 58 mm ($\text{Pb}_4\text{Ga}_4\text{GeS}_{12}$) and 55 mm length ($\text{Pb}_4\text{Ga}_4\text{GeSe}_{12}$) were obtained. It
108 should be noted the lower conical bottom of the selenide sample (up to 2 mm diameter) contains
109 blocs of other phase composition due to the field of the secondary crystallization $\text{L} + \delta + \gamma$. XRD

110 results confirm that the low-temperature modifications of these compounds have non-
 111 centrosymmetric crystal structure (tetragonal symmetry, space group $P\bar{4}2_1c$).

112 Obtained boules were cut using Ni-Cr wire into separate plates that were polished to parallel-
 113 plane, optical quality samples of 0.2 mm thickness. These samples were used for the measurements
 114 of physical properties such as optical absorption and photoconductivity.

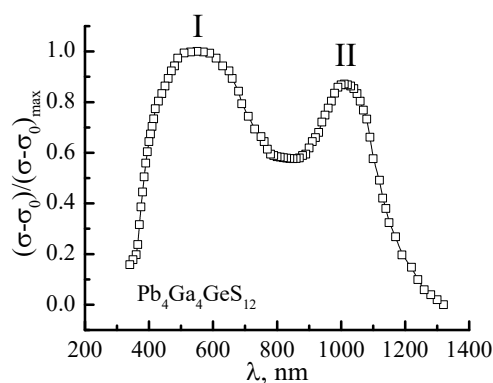
115 The data from experimental absorption spectra (Figure 3) are comparable to the theoretical
 116 calculations of the band gap energy [7]. The band gap of the studied materials was determined by
 117 the extrapolation of the linear part of the absorption curve to the energy axis (Fig. 3 b, d). Obtained
 118 bandgap energy value is equal to 2.28 eV and 1.86 eV for $Pb_4Ga_4GeS_{12}$ and $Pb_4Ga_4GeSe_{12}$ crystals,
 119 respectively, which is close to the results of [1].

120 A study of the spectral distribution of photoconductivity for $Pb_4Ga_4GeS_{12}$ and $Pb_4Ga_4GeSe_{12}$
 121 crystals was undertaken for additional confirmation of obtained results (Figure 4). Experimental
 122 measurements were performed using Keithley 6514 Sub-Femtoamp SourceMeter electrometer.
 123 Sensitivity of experimental setup was not worse than 1 pA. An MDR-206 monochromator with the
 124 diffraction grating with 600 lines/mm and spectral resolution 0.2 nm was used as a spectral device.
 125 The electrical contacts were applied by fusing of Ga-In eutectic and were ohmic for all considered
 126 compositions.

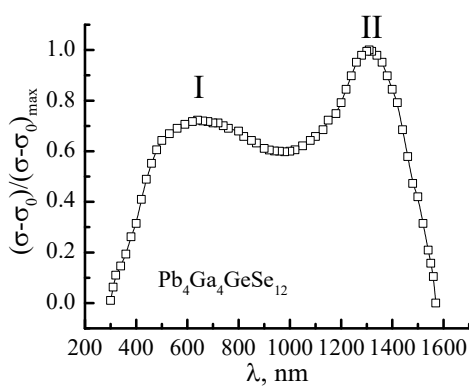


127

128 **Figure 3.** Typical absorption spectra (a, c) versus photon energy and extrapolated (b, d) spectra for
 129 the $Pb_4Ga_4GeS_{12}$ and $Pb_4Ga_4GeSe_{12}$ samples.



130



131

132 **Figure 4.** Spectral distribution of photoconductivity for the $\text{Pb}_4\text{Ga}_4\text{GeS}_{12}$ and $\text{Pb}_4\text{Ga}_4\text{GeSe}_{12}$ crystals.

133 A characteristic feature of the spectral distribution of photoconductivity is the presence of two
 134 spectral maxima. The first lies in the region of $\lambda_1=570$ nm (2.17 eV) and 680 nm (1.82 eV) for the
 135 $\text{Pb}_4\text{Ga}_4\text{GeS}_{12}$ and $\text{Pb}_4\text{Ga}_4\text{GeSe}_{12}$ crystals, respectively, and show a good match with the band gap
 136 estimated from the spectral dependence of the absorption coefficient. Therefore, we can assert that
 137 the peak I of the spectral dependence $\Delta\sigma/\Delta\sigma_{\text{max}}$ is due to the intrinsic photoconductivity of the studied
 138 crystals. The impurity level is located in the region of $\lambda_2=1030$ nm (1.20 eV) and 1340 nm (0.92 eV) for
 139 $\text{Pb}_4\text{Ga}_4\text{GeS}_{12}$ and $\text{Pb}_4\text{Ga}_4\text{GeSe}_{12}$ crystals respectively. One can see from obtained results that the
 140 location of impurity maximum satisfactorily agrees well with the calculated energy positions of
 141 intrinsic defects V_{S} and V_{Se} [7] which is close to the center of the band gap. The lower formation energy
 142 of V_{Se} in comparison with the energy of V_{S} formation favours the prevalence of the peak II of the
 143 impurity photoconductivity in the $\text{Pb}_4\text{Ga}_4\text{GeSe}_{12}$ crystals.

144 **Author Contributions:** Conceptualization, L.P. and H.M.; methodology, L.P., Y.K. and H.M.; sample synthesis,
 145 H.B. and O.N.; single crystal growth, Y.K. and H.B.; DTA and XRD data collection and analysis, Y.K. and H.B.;
 146 optical absorption and photoconductivity data collection and analysis, O.N. and H.M.; writing – original draft
 147 preparation, H.B., Y.K. and O.N.; writing – review and editing, Y.K., L.P. and H.M.; supervision, H.M.; project
 148 administration, L.P. All authors have read and agreed to the published version of the manuscript.

149 **Funding:** This research received no external funding.

150 **Conflicts of Interest:** The authors declare no conflict of interest.

151 References

- 152 1. Chen Y.K.; Chen M.C.; Zhou L.J.; Chen L.; Wu L.M. Syntheses, structures, and nonlinear optical properties
 153 of quaternary chalcogenides: $\text{Pb}_4\text{Ga}_4\text{GeQ}_{12}$ (Q = S, Se). *Inorg Chem.* **2013**, *52*, 8334–8341.

- 154 2. Luo, Z.-Z.; Lin, C.-S.; Cui, H.-H.; Long, W. PbGa₂MSe₆ (M = Si, Ge): Two Exceptional Infrared Nonlinear
155 Optical Crystals. *Chem. Mater.* **2015**, *27*, 914–922.
- 156 3. Fedorchuk, A.O.; Parasyuk, O.V.; Cherniushok, O.; Andriyevsky, B.; Myronchuk, G.L.; Khyzhun, O.Y.;
157 Lakshminarayana, G.; Jedryka, J.; Kityk, I.V.; El-Naggar, A.M.; Albassam, A.A.; Piasecki, M. PbGa₂GeS₆
158 crystal as a novel nonlinear optical material: Band structure aspects. *J. Alloys. Compds.* **2018**, *740*, 294–304.
- 159 4. Yousaf, N.; Khan, W.; Khan, S.H.; Yaseen, M.; Laref, A.; Murtaza, G. Electronic, optical and thermoelectric
160 properties of SnGa₂GeX₆ (X = S, Se) compounds. *J. Alloys Compds.* **2018**, *737*, 637–645.
- 161 5. Huang, Y.-Z.; Zhang, H.; Lin, C.-S.; Cheng, W.-D.; Guo, Z.; Chai, G.-L. PbGa₂GeS₆: An Infrared
162 Nonlinear Optical Material Synthesized by an Intermediate-Temperature Self-Fluxing Method. *Cryst.*
163 *Growth Des.* **2018**, *18*, 1162–1167.
- 164 6. Vilke, K.-T. *Crystal Growth*, Nedra; Leningrad, Russia, 1977.
- 165 7. Piasecki, M. (Jan Dlugosz University, Czestochowa, Poland); Rudysh, M. (Ivan Franko National University
166 of Lviv, Lviv, Ukraine). Personal communication, 2019.
- 167



© 2020 by the authors. Submitted for possible open access publication under the terms and conditions of the Creative Commons Attribution (CC BY) license (<http://creativecommons.org/licenses/by/4.0/>).